Destabilization of the medial meniscus and cartilage scratch murine model of accelerated osteoarthritis

Dunning, Lynette; McCulloch, Kendal; Lockhart, John C.; Goodyear, Carl S.; Huesa, Carmen

Published in:
Journal of Visualized Experiments

DOI:
10.3791/64159

Published: 06/07/2022

Document Version
Publisher's PDF, also known as Version of record

jove

Destabilization of the Medial Meniscus and Cartilage Scratch Murine Model of Accelerated Osteoarthritis

Lynette Dunning[1], **Kendal McCulloch**[1], **John C. Lockhart**[1], **Carl S. Goodyear**[2], **Carmen Huesa**[2]

[1] Institute of Biomedical and Environmental Health Research, University of the West of Scotland [2] Institute of Infection, Immunity and Inflammation, University of Glasgow

Corresponding Author

Carmen Huesa
carmen.huesa@glasgow.ac.uk

Citation

Dunning, L., McCulloch, K., Lockhart, J.C., Goodyear, C.S., Huesa, C. Destabilization of the Medial Meniscus and Cartilage Scratch Murine Model of Accelerated Osteoarthritis. *J. Vis. Exp.* (185), e64159, doi:10.3791/64159 (2022).

Date Published

July 6, 2022

DOI

10.3791/64159

URL

jove.com/video/64159

Abstract

Osteoarthritis is the most prevalent musculoskeletal disease in people over 45, leading to an increasing economic and societal cost. Animal models are used to mimic many aspects of the disease. The present protocol describes the destabilization and cartilage scratch model (DCS) of post-traumatic osteoarthritis. Based on the widely used destabilization of the medial meniscus (DMM) model, DCS introduces three scratches on the cartilage surface. The current article highlights the steps to destabilize the knee by transecting the medial meniscotibial ligament followed by three intentional superficial scratches on the articular cartilage. The possible analysis methods by dynamic weight-bearing, microcomputed tomography, and histology are also demonstrated. While the DCS model is not recommended for studies that focus on the effect of osteoarthritis on the cartilage, it enables the study of osteoarthritis development in a shorter time window, with special focus on (1) osteophyte formation, (2) osteoarthritic and injury pain, and (3) the effect of cartilage damage in the whole joint.

Introduction

Osteoarthritis (OA) is the most prevalent musculoskeletal disease in people over 45, with over 8.75 million seeking treatment in the UK[1]. The growing prevalence of the disease has led to an increased economic and societal cost, is a major contributor to disability, and reduces the quality of life for patients[1]. Without treatments available, there is an urgent need to accelerate research to understand the development and progression of the disease. The disease is complex and also multifactorial in its nature. The main clinical measurements of the disease are pain and joint mobility[2], and OA affects all the tissues in the joint, not just the cartilage[3]. One of the main challenges in understanding OA is that it can take years, sometimes decades, from initial presentation/injury to symptomatic disease progression with pain and immobility.

Modeling osteoarthritis in rodents has enhanced our knowledge of OA pathophysiology by allowing us to

understand the initiation and progression in a much shorter time frame and with a detailed examination of the tissues involved. There are numerous murine models of osteoarthritis, from genetically modified animals to surgical intervention models. The most widely used murine model of post-traumatic OA is the destabilization of the medial meniscus (DMM)[4,5]. A caveat of the model is the variability between different operators. Experienced surgeons can perform the procedure with minimal joint damage, while inexperienced operators expose the joint capsule for longer periods of time and inflict damage on the cartilage. This variability in the process influences the severity of the model, with more initial damage leading to increased cartilage damage scores and osteophyte formation. Intending to reduce the variability between operators and mimic cartilage damage from clinical intervention, a modified version of this model is developed, whereby controlled additional damage onto the cartilage surface in the form of three superficial scratches are inflicted[6]. This also allows modeling the OA progression resulting from cartilage damage caused by some clinical interventions. Compared to the standard DMM model, the directly induced cartilage damage results in consistently accelerated protruding osteophyte formation, increased cartilage damage and inflammation, and measurable surrogate pain in male mice.

This model is particularly suitable for the study of early-stage post-traumatic OA, focusing on osteophyte formation, pain presentation (in male mice), synovitis, and early changes to bone parameters. The consistency of osteophyte formation in this model makes it pertinent to study bone repair and endochondral ossification since osteophyte formation is a process of repair *via* endochondral ossification[7]. The model also mimics damage introduced directly to the cartilage during clinical interventions, such as arthroscopic surgical procedures, and thus it is also suitable for the study of the effect of cartilage damage on the whole joint.

Protocol

All experimental procedures were approved by the Ethical Review Panel of the University of Glasgow and the University of the West of Scotland, and carried out following the Animals (Scientific Procedures) Act 1986 (UK) guidelines. 10-week-old C57Bl6/J male mice, weighing around 25 g, were used for the present study. The mice were obtained from commercial sources (see **Table of Materials**).

1. Animal preparation

NOTE: Consider mouse gender in regards to the purpose of the study as post-traumatic OA models display important differences depending on gender[8,9,10].

1. Ensure that the anesthetic reagent (2% isoflurane) is ready.

   NOTE: Injectable anesthesia can also be used[11]. Given the quick duration of the surgery, the use of inhalant anesthesia is recommended.

2. Use a separate sham-operated age-matched group as surgical control.

   NOTE: The contralateral knee must not be used as a surgical control (sham operation on the contralateral leg). This may have issues in terms of animal welfare, and it will likely affect gait and gait measurements. The contralateral knee normalizes intrinsic bone parameters[12] and acts as a paired comparison on evoked pain tests[13].

3. Use skeletally mature mice.

NOTE: Most literature induces OA at 8-12 weeks of age. In the present study, the mice are 10 weeks old.

2. Pre-operative care (carried out by a surgical assistant)

1. If transported from a different facility, allow at least 1 week prior to surgical intervention for mice to adjust to their new environment.
2. Carry out surgery in an appropriately designated sterile room, ensuring all surfaces are sterile (e.g., use sterile drapes to cover areas of surgery).
   NOTE: The surgery is aseptic.
3. Arrange and place sterile instruments on sterile drapes.
4. Weigh the mouse.
5. Induce anesthesia by introducing the mouse in an anesthetic cage and then introducing 2% isofluorane for upto 15 min using a standard anesthetic rig (see **Table of Materials**).
   NOTE: The cage must not have "residual" anesthesia prior to introducing the mouse.
6. Once anesthetized, take the mouse out of the anesthetic chamber and clip the fur over the knee, front and lateral sides from the mid-shin to the mid-thigh with small hair clippers.
   NOTE: The choice of hindlimb knee is up to the operator's preference on which side they find easier to conduct the surgery. This protocol operated on the left leg.
7. Ensure the mouse is fully anesthetized (non-responsive to pinching the foot).
8. Disinfect skin by applying antibacterial skin cleanser (e.g., containing chlorhexidine or iodophor, see **Table of Materials**) on shaved exposed skin.
9. For analgesia, administer 0.05 mg/kg of buprenorphine subcutaneously.
10. Place the mouse on the dorsal side, leaving the knee to be operated on upwards, and place the mouse nose in the nozzle connected to the anesthetic rig.
11. Cover the mouse with a sterile drape with a small keyhole opening.
12. Position the leg to be operated on with the knee flexed at less than 90°, with the patellar ligament facing upwards and the foot immobilized with surgical tape.

3. Destabilization of the medial meniscus procedure followed by cartilage scratch

1. Adjust the microscope to focus on the patellar ligament.
2. Pinch the skin of the knee on the lateral side with serrated forceps (see **Table of Materials**), make a small cut parallel to the distal patellar tendon using surgical scissors, introduce the scissors and expand the cut to about 1 cm. Move the skin over to the medial side, exposing the patellar ligament and the proximal tibial plateau (**Figure 1**).
3. With a number 11 blade, make an incision along the medial side of the patellar ligament, from the top to the bottom of the ligament (**Figure 1A**). When reaching the bottom of the patellar ligament, turn the blade 90° and extend the incision away from the patellar ligament toward the medial side to gain access to the joint capsule.
   NOTE: Bleeding may occur in this or the subsequent steps. If bleeding occurs use a sterile cotton bud and apply pressure a few seconds (5 to 30 s).
4. Pinch the patellar ligament with blunt tip forceps and rotate the wrist to move the patellar ligament to the lateral side, just enough to expose the infrapatellar fat pad (IFP).

NOTE: To minimize damage to the patellar ligament, do not hold the tweezers too tight, just sufficient to keep the ligament to the side.

5. While still holding the patellar ligament lightly, pinch the IFP with micro-tweezers (see **Table of Materials**) to raise it and move it slightly upward. This allows visualizing the medial meniscus ligament.

6. Identify the medial meniscotibial ligament (MMTL) of the medial meniscus, which anchors the cranial horn of the medial meniscus to the anterior tibial plateau (**Figure 1B**).

7. Avoid damage and prolonged cartilage exposure at the tibial plateau or femoral condyle.

8. Carefully sever the MMTL with small 2 mm blade Vannas spring scissors, leaving the medial meniscus and other ligaments intact. At this point, the surgical procedure for the DMM model is completed (**Figure 1C**).

9. With a 3 mm microsurgical knife, mark three evenly spaced indentations on the tibial articular cartilage in a direction from the posterior to the anterior part.
   NOTE: The scores are about 1 mm in length and only damage the surface of the cartilage (**Figure 2D**).
   1. Do not use excessive force with the blade onto the cartilage (i.e., ensure the scratches are superficial). This additional step inflicts cartilage damage, inducing the DCS model.

10. Close the skin with two or three small 7 mm wound closure metal clips or absorbable 6-0 subdermal surgical sutures (see **Table of Materials**).
    NOTE: Subdermal surgical sutures are better as they avoid further intervention, but they extend the surgery duration. External sutures increase the risk of wound opening by the gnawing of the mice.

11. Identify the medial meniscotibial ligament of the medial meniscus for sham surgery, but do not sever.

12. For mice only receiving cartilage scratches, make the three superficial scratches without severing the ligament.
    NOTE: Between each mouse, change gloves and sterilize instruments *via* autoclave. Remember to check the instruments have cooled before re-use.

4. Post-operative care

1. If bleeding has occurred (>50 uL), inject 500 µL of warm sterile saline subcutaneously (on the back of the mouse).
   NOTE: In our experience, although mice have minor bleeds, it never is more than a small drop, and thus fluids do not need to be replenished.

2. After surgery, place the mouse in a recovery cage on a clean paper tissue and allow recovery from anesthesia (5-10 min).

3. Transfer the fully conscious mice into a clean cage with fresh bedding after surgery.

4. In the 72 h after surgical intervention, monitor for any signs of pain or distress. Pay attention to:
   1. Changes in body weight. Although body weight may decrease on the first and second day, this is usually no more than 5% of the pre-surgical body weight.
   2. General lack of grooming or over-grooming around the incision.
   3. Signs of general health deterioration, such as hunched posture, facial grimacing, and/or abnormal respiration.
   4. Wound infection as indicated by any swelling, discharge, or opening of the wound.

NOTE: Infection may occur if the surgical wound opens. As surgical wound repair (e.g., replacing missing metal clips or re-suturing) is a regulated procedure, ensure relevant approval is obtained prior to performing repairs.

5. Remove metal clips between 5-7 days post-surgery.

6. Maintain mice typically 2-52 weeks post-operatively depending on the study design.

7. Evaluate pain/gait at any point during the study.
NOTE: The present study uses dynamic weight-bearing as described in step 5.1.

8. Euthanize the animal by an approved method, according to the national licensing agreements, local guidelines, and experimental approval.
NOTE: In the present study, the animals were euthanized *via* exsanguination (cardiac puncture) under terminal anesthesia followed by cervical dislocation[14].

5. Evaluation of osteoarthritic disease

1. Measure dynamic weight bearing as a surrogate measurement of pain following the steps below.
NOTE: As mice are prey animals, they tend to hide pain behaviors. This makes the measurement of pain difficult. There are many ways to measure evoked pain, such as Von Frey[15] and gait analysis[16]. The present study measured the differential load between the operated osteoarthritic leg and the unoperated control leg on a pressure mat while the mouse was in a cage (see **Table of Materials**, **Figure 2A**).
    1. Weigh the mouse. Tare and calibrate the pressure mat according to manufacturer's specific instructions (see Dynamic weight-bearing equipment in **Table of Materials**). Introduce the mouse in the cage.
    2. Record movement and paw pressure of the mouse in the cage for 5 min. Analyze acquired data to validate 1 min, following manufacturer's instructions.
    NOTE: The manufacturer's automated analysis on DWB software (see dynamic weight-bearing equipment in **Table of materials**) provides measurements on each paw in proportion to the total body weight, the amount of the validated time that each paw remained on the mat, and an estimation of the mat area occupied by each paw. This allows the calculation of the differential load between the two rear paws, the differential load between the front and rear paws, an increase of front paw loading (if the same mouse has been measured over a period of time), the time spent lifting the OA leg in comparison to the contralateral leg and the paw surface.

2. Quantify calcified tissue through microcomputed tomography (μCT).
NOTE: Although subchondral bone osteosclerosis and osteophyte formation can be measured in histological sections, μCT offers the opportunity to quantify three-dimensionally. The resolution of image capture in μCT at 5 μm is sufficient, as this allows visualization of smaller structures such as the osteophytes, although the higher the resolution, the better.
    1. Fix knee joints in 4% paraformaldehyde solution for 24 h, then transfer to 70% EtOH.
    2. Scan knee joints in a μCT scanner.
    NOTE: In the present study, the samples were scanned on a μCT scanner (see **Table of Materials**) with a 0.5 aluminum filter set at 50 kV and 200 μA. Samples were examined at a voxel size of 4.5 μm; 2

μm, 0.2° rotation angle for imaging, and 0.5° rotation angle for quantification.

3. Reconstruct scans to allow 3D visualization. The scans presented here were reconstructed using compatible software (see **Table of Materials**).

4. Analyze subchondral bone sclerosis (**Figure 2B**) following the steps below.

    1. Select a volume of interest (VOI) of 0.5 mm × 0.9 mm × 0.9 mm in the center of the load of the medial tibial plateau[17].

    2. Normalize against the intrinsic bone phenotype of the mouse by analyzing the unoperated leg.

    3. Determine the subchondral bone density and micro-architecture by selecting a region of interest (ROI) delineating the trabecular structure within the tibial epiphysis, the subchondral plate, or the total subchondral bone in the two-dimensional coronal view of the stack using CTan software (see **Table of Materials**).

        NOTE: As the disease progresses, the separation between the subchondral plate and subchondral trabecular region becomes more difficult to distinguish. It is then recommended to analyze the area of subchondral bone selected from the joint space to the growth plate.

5. Quantify osteophytes (**Figure 2C**) following the steps below.

    1. Identify osteophytes in the reconstructed three-dimensional image stacks using CTvol software (see **Table of Materials**).

        NOTE: Mineralized osteophytes are protrusions similar to woven bone visible on the medial side of the subchondral bone[18]. An example of these is indicated with yellow arrows in **Figure 2C**.

    2. Manually count the number of identified osteophytes in the medial side of the knee joint.

    3. Measure osteophyte volume in 2D sequential image analysis (using the CT analyzer) by delineating the edge of osteophytes manually, protruding from the subchondral plate as the region of interest (ROI) for analysis.

    4. Calculate osteophyte bone density as the ratio of bone volume over osteophyte volume using the CT analyzer software (see **Table of Materials**).

3. Evaluate cartilage damage and synovitis (**Figure 2D**) according to the OARSI cartilage damage score[19] and synovitis score[20] on paraffin-embedded 6 μm sections.

    1. After scanning, decalcify knee joints in 10% EDTA at 4 °C for a minimum of 2 weeks, changing solution twice a week.

    2. Embed samples in paraffin. For treatments and incubation periods, see **Supplementary File 1**.

    3. Cut 5 μm coronal sections of paraffin-embedded samples on a rotary microtome (see **Table of Materials**).

    4. Select sections in the area where the tibial and femoral condyles meet (**Figure 2D**). Select two sections in three equally distanced areas of the joint.

        NOTE: Sections scored in the present study were selected in areas 80-100 μm apart.

    5. Stain sections with Safranin-O and Fast green (see **Table of Materials**) following the steps below.

1. Deparaffinize sections by submerging them (in the mentioned sequence) in Xylene for 5 min (2x), 100% ethanol for 2 min, 95% ethanol for 2 min, 80% ethanol for 2 min, and 70% ethanol for 2 min.
2. Stain with filtered Haematoxylin (see **Table of Materials**) for 30 s. Then rinse in tap water for 5 min (three times).
3. Wash with Scott's buffer (2 g of sodium bicarbonate and 10 g of magnesium sulfate in 1 L of distilled water) for 2 min. Rinse in 'tap water' for 5 min (three times).
4. Stain for 4 min with 0.2% Fast green. Dip in 1% glacial acetic acid, five times (freshly made each session). Rinse quickly in tap water.
5. Stain for 5 min with 0.5% Safranin-O. Rinse in 95% ethanol. Dehydrate sections in 100% ethanol for 3 min followed by 3 min in Xylene.
6. Score sections as stated in Glasson et al. for cartilage[19] and Jackson et al. for synovitis[20].
   NOTE: Other methods of quantification exist, such as the computer-based quantification by Pinamont et al.[21].
7. Validate the scoring system with two different scorers, blinded to the experiment.

Representative Results

The percentage load per total body weight of the rear operated/OA leg was compared to the contralateral/control leg. Although other parameters may also give significant differences, like the increase in front paw load after surgical intervention, a consistent change in rear paw load indicates a preference to use one leg over the other and is a more direct indicator of significant discomfort for the mouse due to OA development. There were no significant changes in rear leg load in the DMM model within 8 weeks post-induction, while DCS mice favor the contralateral/control leg significantly 2 weeks after intervention (**Figure 3A**).

Subchondral bone was analyzed by focusing on the volume under the medial loaded region of the tibial condyle. Here we assessed the bone density of this area by determining the percentage of mineralized bone within the region of interest and calculated the ratio between the contralateral and the ipsilateral leg. The ratio indicates that both models have increased bone density in the affected limb (ratio above 1) 4 weeks after induction (**Figure 3B**). The emergence of osteophytes is more prominent in the DCS model, where there is a significant increase in the number and volume compared to the DMM model 2 weeks after intervention (**Figure 3C,D**). DCS presents elevated cartilage damage in the medial tibial and femoral compartments and synovitis (**Figure 3E,F**) 4 weeks after induction.

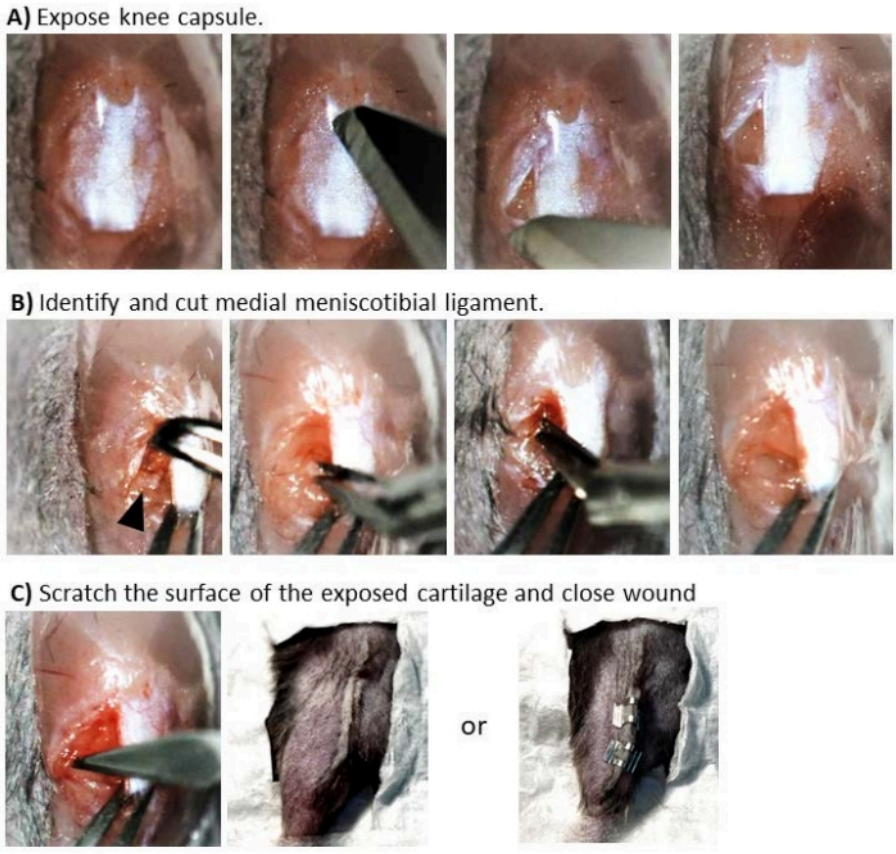

Figure 1: Surgical intervention to induce post-traumatic OA in the mouse. Sequential images represent the different stages of the procedure. (**A**) Exposure of joint capsule cutting the superficial membrane around the knee by inserting a number 11 scalpel blade on the medial side of the patellar ligament and away from the ligament. This will expose the infrapatellar fat pad. (**B**) Identification and transection of the medial meniscotibial ligament. To identify the ligament, move the patellar ligament toward the lateral side and then push the fat pad upward. This allows for the visualization of the ligament as a small horizontal white line just above the tibial condyle (indicated here with a black arrow). To cut the ligament, the lower blade of the spring scissors is placed under the ligament, taking care not to damage the cartilage. Move the meniscus towards the medial side to visualize the tibial condyle. (**C**) Scratching the surface of the exposed cartilage and closure of the wound. To scratch the cartilage, the microblade is inserted toward the posterior side, where it contacts the cartilage and then moves forward toward the anterior part of the joint. Once the scratches are done, pull the skin over the knee and close the wound either by subdermal suturing or with wound clips. Please click here to view a larger version of this figure.

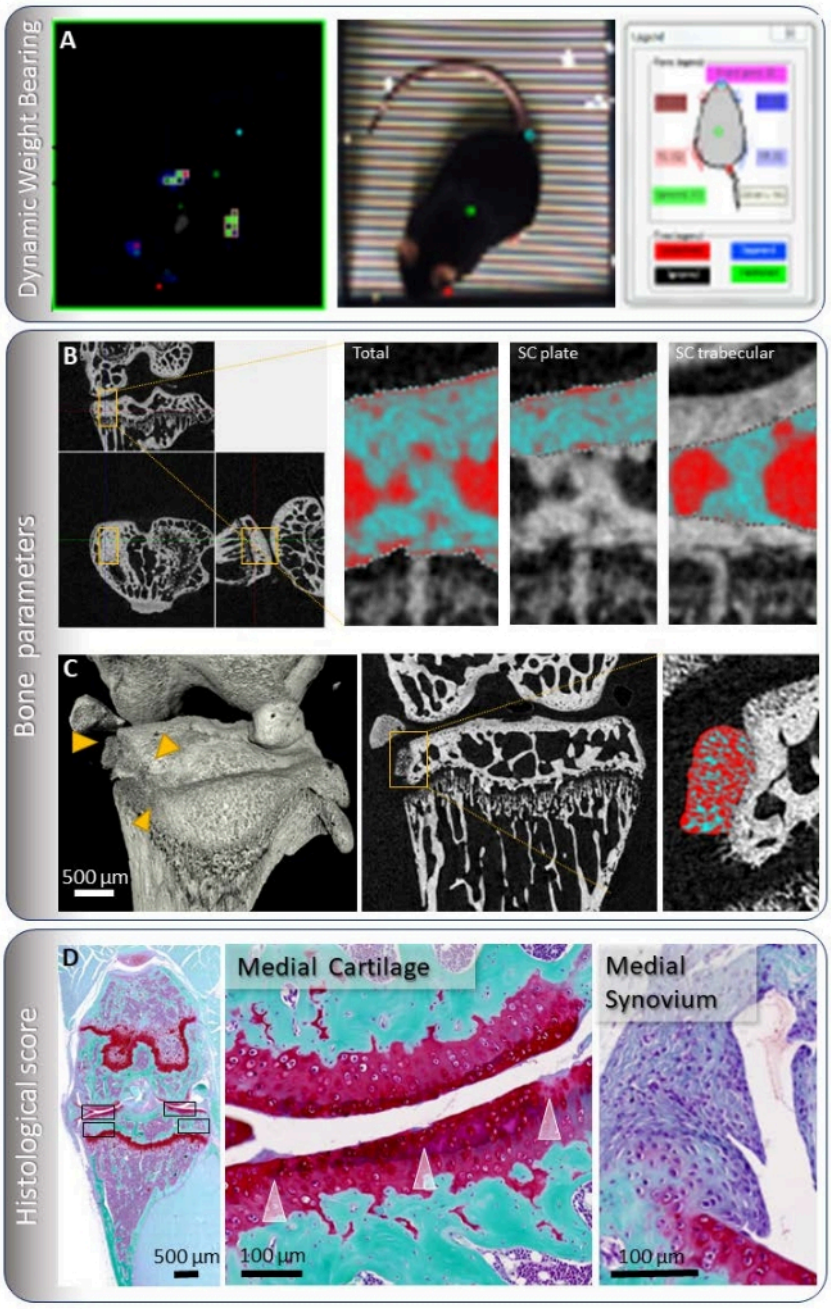

Figure 2: Evaluation of osteoarthritis in the mouse. (**A**) Dynamic weight-bearing consists of matching the load on a pressure mat to the corresponding paw. The load is then expressed as a percentage of the total weight. (**B**) Subchondral bone is measured by selecting a volume of interest in the loading region of the medial tibial condyle and selecting the subchondral plate or trabecular bone. These images are at a resolution of 4.5 µm. (**C**) Osteophytes are identified and quantified in a three-dimensional view of the acquired µCT images. The volume of osteophytes is measured by selecting an ROI delineating the edge of the osteophyte. The bone density is calculated as the bone volume per osteophyte volume. The

images presented here were taken at a resolution of 2 µm, but quantification is usually done with a 4.5 µm resolution. (**D**) Cartilage and synovitis scores are taken from 6 µm sections stained with Safranin-O and Fast green. A coronal section of the mouse knee where all quadrants, marked with a black box, are visible for scoring and a magnification of the medial side is shown. The synovitis surrounding the medial side of the knee joint is also visible, especially above and below the displaced meniscus. Please click here to view a larger version of this figure.

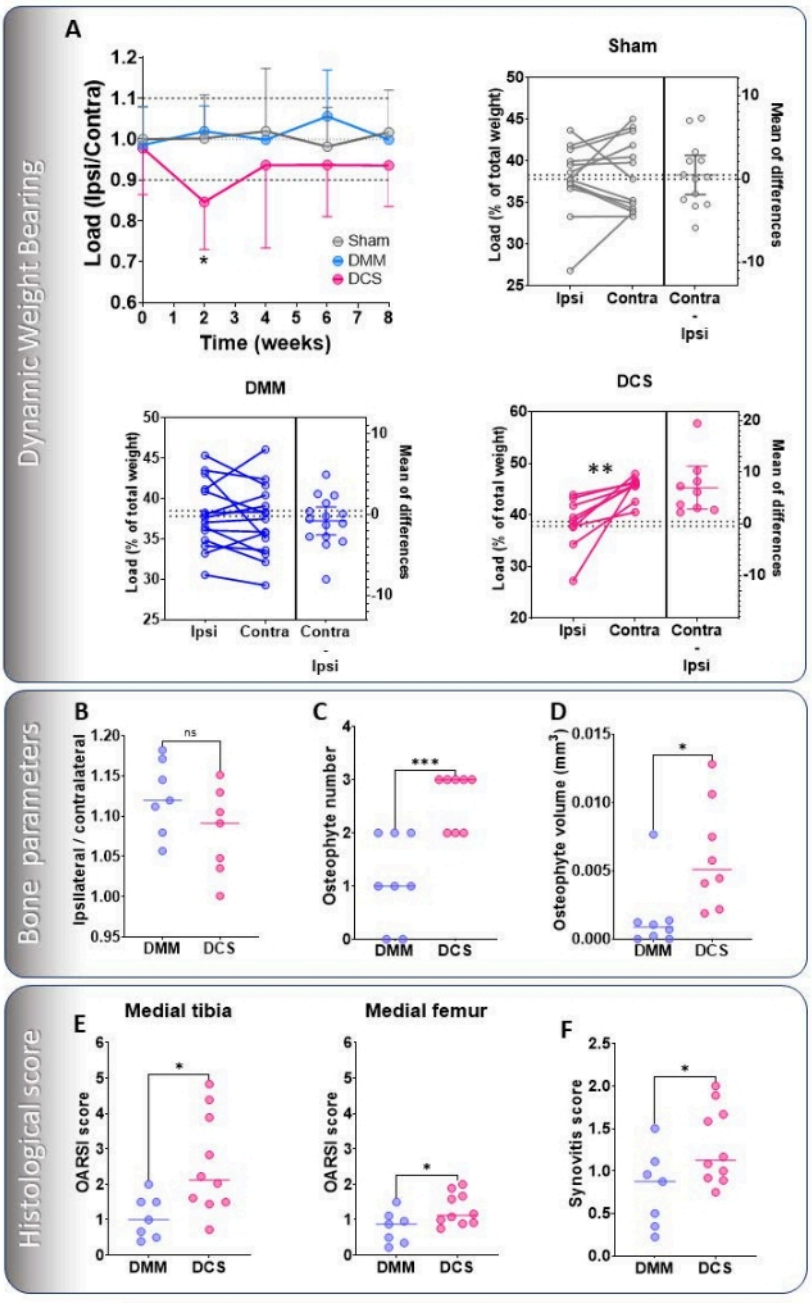

Figure 3: Representative evaluation of OA in the DMM and the DCS models. (**A**) DWB measured up to 8 weeks post-induction on experiments carried out by the same expert operator. Load is expressed as a ratio between the operated/OA load versus the contralateral/control load. Paired t-tests of both legs are also shown in the Sham (grey), DMM (blue), and DCS (pink) models. µCT analysis 4 weeks after surgical intervention. (**B**) Subchondral bone was analyzed 4 weeks after surgical intervention and expressed as the ratio of the ipsilateral over the contralateral %BV/TV. (**C**) Osteophyte number and (**D**) osteophyte volume was analyzed 2 weeks after induction. Histological evaluation 4 weeks after induction of (**E**) cartilage

damage of the medial tibial and femoral articular cartilage and (**F**) synovitis were scored with standardized methods[19,20]. Data are expressed as mean ± standard deviation, n ≥ 5. Data were compared by repeated-measures ANOVA with a Šídák test correction (**A**), paired t-test (**A**), or standard Student's t-test (**B-F**). *P < 0.05, **P < 0.01, ***P < 0.001, ns = not significant. Please click here to view a larger version of this figure.

Supplementary File 1: Treatment and incubation condition for paraffin embedding. Please click here to view a larger version of this figure.

Discussion

To perform surgical induction of post-traumatic osteoarthritis (PTOA), support from an assistant is strongly recommended (e.g., to prepare the mice while the operator focuses on the surgery). This facilitates aseptic surgery, thereby reducing the risks of infections and making the intervention more efficient in large experiments. It is easy to lose the plane of focus during the surgery, so a microscope that includes pedals for focusing is a valuable feature in helping to maintain sterility throughout the surgery. The position of the mouse and the knee is crucial. The knee must be facing upward and sufficiently bent to maximize the opening of the knee joint space, facilitating easier access to the ligament for introducing the microblade to scratch the condyle surface. Identifying the MMTL can be challenging, especially when the fat pad is larger than usual or there is a small bleed. To avoid bleeds, push the fat pad upward to prevent tears and subsequent bleeding. If the fat pad is large, this might take a little longer, but patiently continue to push it upwards.

The MMTL is quite close to the tibial condyle, so one must take care not to injure the cartilage when positioning the lower blade of the curved spring scissors under the MMTL. The curved blades should point toward the medial side and slightly upward, parallel to the condyle. For best sectioning of the MMTL, ensure the scissors are sharp. Check that the meniscus can move medially after cutting the ligament, as sometimes a small attachment remains that needs further cutting. When introducing the microblade to scratch the condyle, it must be perpendicular to the condyle. Make the first scratch closer to the middle of the joint but take care not to damage the anterior cruciate ligament. Then move toward the medial side and then behind the meniscus. The scratches might be visible as faint white lines on the cartilage. Because we usually use clips, the initial incision is performed on the lateral side, so the clips are positioned on the side of the leg after closing the wound. This avoids the clips rubbing the knee as the mouse regains movement. When using sutures, the use of subdermal stitches is strongly recommended. If using external stitches, the mice are likely to gnaw at the stitches and open their wound, which will increase the chances of infection. When done right, this surgery must not take more than 5-10 min, from incision to wound closure, thus minimizing the exposure of the cartilage and any additional uncontrolled damage that may occur. After the surgery, the mice recover very quickly and almost immediately can climb into the cage and move around normally. If the mice are not active, the appropriate expert in the unit should be consulted.

For the behavioral evaluation of pain, dynamic weight-bearing was assessed. However, this method may be considered less sensitive than other evoked pain tests, such as von Frey testing[15]. It is recommended that more than one method is used to monitor and assess pain. The changes observed 2 weeks after intervention in DCS, even though transient, indicate a generally decreased loading of the OA leg compared to the healthy leg. Therefore, 2 weeks

after DCS intervention may be used to evaluate early osteoarthritic or injury pain in mouse models. Visualization of mineralized osteophytes by μCT allows for three-dimensional quantification, which can also be matched to the histological sections[12], adding another dimension to the study of osteophyte emergence and evolution. In our group, osteophyte presence was variable in the DMM model between and within operators (2.3 ± 1 *vs*. 1.2 ± 1, n > 7, *P* = 0.0183), whereas induction of DCS robustly led to osteophyte generation in all cases irrespective of the operator (2.6 ± 0.7 *vs*. 2.4 ± 0.5, n > 7, *P* = 0.711). Also, there are significantly more and larger osteophytes in the DCS model compared to DMM. Thus, DCS is an ideal model for the study of osteophyte formation. Quantification of osteosclerosis limited to the loading area of the subchondral bone is also an improvement in detecting small changes. Comparing the medial compartment of the operated leg to the contralateral leg also offers a way to normalize against the intrinsic bone phenotype of that particular mouse[12]. The addition of the cartilage scratches in the DCS model is a controlled means of inducing focused cartilage damage during surgery that accelerates many of the aspects of the disease. One of the consequences of the experimental procedure involving intentional damage to the cartilage itself is that this artefactual damage needs to be excluded or adjusted for in the cartilage grading system. Because of this limitation, we do not recommend this model if the study's main aim is to understand the effect of osteoarthritis on the cartilage itself. Finally, it is also strongly recommended to have at least two blinded scorers grade the cartilage damage and synovitis scores. This validates and enhances the standardization of the scoring systems.

A limitation of this study is that the extent of variability across all the parameters comparing the DCS and DMM models was not fully evaluated. This will be addressed in the future with more extensive studies, which could also include an assessment of the variability between operators from different institutions.

In conclusion, the accelerated OA pathogenesis in the current DCS model allows representation of post-traumatic OA and provides a powerful and robust research tool to investigate and elucidate underlying OA pathophysiological mechanisms driving this chronic debilitating joint disease. Additionally, it enables OA to be explored in a shorter time window, focusing on osteophytogenesis, OA pain, and the effect of cartilage damage on the whole joint.

Disclosures

The authors have nothing to disclose.

Acknowledgments

We would like to acknowledge the work of Gemma Charlesworth and Mandie Prior at the University of Liverpool, who acquired the μCT images used in this publication. Work was funded by Versus Arthritis (grants 20199 and 22483). Lynette Dunning was funded by Versus Arthritis (grant 20199). Kendal McCulloch was funded by a UWS PhD scholarship. Carmen Huesa was funded by Versus Arthritis (grants 20199 and 22483).

References

1. Arthritis Research UK. *The State of Musculoskeletal Health 2018*. 30 (2018).
2. Mahir, L. et al. Impact of knee osteoarthritis on the quality of life. *Annals of Physical and Rehabilitation Medicine.* **59**, e159 (2016).

3. Chen, D. et al. Osteoarthritis: toward a comprehensive understanding of pathological mechanism. *Bone Research.* **5**, 16044 (2016).
4. Glasson, S. S., Blanchet, T. J., Morris, E. A. The surgical destabilization of the medial meniscus (DMM) model of osteoarthritis in the 129/SvEv mouse. *Osteoarthritis and Cartilage.* **15** (9), 1061-1069 (2007).
5. Sophocleous, A., Huesa, C. Osteoarthritis mouse model of destabilization of the medial meniscus. *Methods in Molecular Biology.* **1914**, 281-293 (2019).
6. McCulloch, K. et al. Accelerated post traumatic osteoarthritis in a dual injury murine model. *Osteoarthritis and Cartilage.* **27** (12), 1800-1810 (2019).
7. Fan, X., Wu, X., Crawford, R., Xiao, Y., Prasadam, I. Macro, micro, and molecular. changes of the osteochondral interface in osteoarthritis development. *Frontiers in Cell and Developmental Biology.* **9**, 659654 (2021).
8. Hwang, H. S., Park, I. Y., Hong, J. I., Kim, J. R., Kim, H. A. Comparison of joint degeneration and pain in male and female mice in DMM model of osteoarthritis. *Osteoarthritis and Cartilage.* **29** (5), 728-738 (2021).
9. Loga, I. S. et al. Does pain at an earlier stage of chondropathy protect female mice against structural progression after surgically induced osteoarthritis? *Arthritis & Rheumatology.* **72** (12), 2083-2093 (2020).
10. Ma, H. L. et al. Osteoarthritis severity is sex dependent in a surgical mouse model. *Osteoarthritis and Cartilage.* **15** (6), 695-700 (2007).
11. Cicero, L., Fazzotta, S., Palumbo, V. D., Cassata, G., Lo Monte, A. I. Anesthesia protocols in laboratory animals used for scientific purposes. *Acta Biomedica.* **89** (3), 337-342 (2018).
12. Huesa, C. et al. Proteinase-activated receptor 2 modulates OA-related pain, cartilage and bone pathology. *Annals of the Rheumatic Diseases.* **75** (11), 1989-1997 (2016).
13. Tappe-Theodor, A., King, T., Morgan, M. M. Pros and cons of clinically relevant methods to assess pain in rodents. *Neuroscience and Biobehavioral Reviews.* **100**, 335-343 (2019).
14. Stewart, K., Schroeder, V. A. Lab animal research. blood withdrawal I. *JoVE Science Education Database, Cambridge, MA.* (2018).
15. Chaplan, S. R., Bach, F. W., Pogrel, J. W., Chung, J. M., Yaksh, T. L. Quantitative assessment of tactile allodynia in the rat paw. *Journal of Neuroscience Methods.* **53** (1), 55-63 (1994).
16. Lakes, E. H., Allen, K. D. Gait analysis methods for rodent models of arthritic disorders: reviews and recommendations. *Osteoarthritis and Cartilage.* **24** (11), 1837-1849 (2016).
17. Das Neves Borges, P., Forte, A. E., Vincent, T. L., Dini, D., Marenzana, M. Rapid, automated imaging of mouse articular cartilage by microCT for early detection of osteoarthritis and finite element modelling of joint mechanics. *Osteoarthritis and Cartilage.* **22** (10), 1419-1428 (2014).
18. van der Kraan, P. M., van den Berg, W. B. Osteophytes: relevance and biology. *Osteoarthritis and Cartilage.* **15** (3), 237-244 (2007).
19. Glasson, S. S., Chambers, M. G., Van Den Berg, W. B., Little, C. B. The OARSI histopathology initiative

- recommendations for histological assessments of osteoarthritis in the mouse. *Osteoarthritis and Cartilage.* **18** (SUPPL. 3), S17-S23 (2010).

20. Jackson, M. T. et al. Depletion of protease-activated receptor 2 but not protease-activated receptor 1 may confer protection against osteoarthritis in mice through extracartilaginous mechanisms. *Arthritis and Rheumatology.* **66** (12), 3337-3348 (2014).
21. Pinamont, W. J. et al. Standardized histomorphometric evaluation of osteoarthritis in a surgical mouse model. *Journal of Visualized Experiments.* **159**, e60991 (2020).